



 Cite this: *RSC Adv.*, 2020, 10, 34373

# Effect of ethylene glycol and its derivatives on the aggregation properties of reactive Orange 13 dye aqueous solution

 Yong Qi,† Ruyi Xie,† Aihong Yu, Mohd Nadeem Bukhari, Liyuan Zhang, Chuangui Cao, Hui Peng, Kuanjun Fang\* and Weichao Chen \*

The aggregation behavior of dyes especially in the dyeing and printing of different textile materials is an important phenomenon which affects the process of dye adsorption and diffusion. In order to avoid the aggregation of dyes, scientists are looking for materials which can inhibit the aggregation process by fabricating the dye solution. Organic solvents have found important influence in the aggregation of dye molecules. Therefore, herein, we report the fabrication of reactive orange 13 dye solutions with the aid of ethylene glycol and its derivative organic solvents to investigate the aggregation behavior of dye molecules by UV-vis absorption spectrum, fluorescence spectrum, surface tension, rheological and particle size measurements. IR spectra were performed to understand the effect of hydrogen bonding on the aggregation behavior of dye molecules. Moreover, transmission electron microscopy was also tested to confirm the effect of organic solvents on the surface morphology of dye molecules. The results show that the reactive Orange 13 dye molecules show aggregation in terms of dimeric and multimeric structures at high dye concentrations due to  $\pi$ - $\pi$  interaction of naphthalene rings. Moreover, on introducing the ethylene glycol and its derivatives, the dye molecules disaggregate by hydrophobic interactions of dye molecules and organic solvents which destroyed the ice-like structure between the dye molecules and the water molecules. Among the three organic solvents, DME solvent caused more disaggregation of reactive Orange 13 dye molecules due to extra hydrophobic methyl groups in its structure. The results also show that the interaction between Orange 13 dyes and ethylene glycol and its derivatives could decrease the surface tension and particle size of the dye, and increase the quantum yield and viscosity. This research will help to understand the aggregation behavior of dyes and help the textile industries to choose the suitable formulations of dye solutions for coloration of different textile substrates *via* dyeing and printing methods.

 Received 21st July 2020  
 Accepted 8th September 2020

DOI: 10.1039/d0ra06330d

[rsc.li/rsc-advances](http://rsc.li/rsc-advances)

## Introduction

Research on the aggregate structure of dyes especially in favourable areas like solar power generation (cyanine dyes),<sup>1-4</sup> dyeing and printing<sup>5-8</sup> has always remained a hot topic for researchers to work on so that a number of problems can be eliminated. In particular, the aggregation behaviour of dyes creates a problem in the preparation of homogeneous dye solutions or inks for dyeing and printing of different textile substrates through affecting the process of dye adsorption and diffusion. The aggregate degree is associated with the structure of dye molecules. Generally, dyes with better molecular planarity are more likely to form aggregates.<sup>9,10</sup> Reactive dyes are

the colours of choice to print cotton fabrics due to their bright colour, excellent applicability and wide colour gamut.<sup>11-13</sup> However, reactive dyes are prone to aggregate in aqueous solution especially at high concentration,<sup>14</sup> which can affect the fixation rate of the finished product. The surface tension and viscosity of the dye solutions are also two important parameters which can influence on the dyeing and printing.<sup>15</sup> Adding a suitable organic solvents to the dye solution could improve the quality of inkjet printing<sup>10,16</sup> by not only increases the solubility of dye molecules but also adjusting the surface tension and viscosity parameters. Therefore, it is of primary importance to study the interaction mechanism between the organic solvents and reactive dyes.

The aggregation behaviour of dyes is affected by many factors. Increasing temperature,<sup>17,18</sup> reducing salt<sup>19,20</sup> and adding urea<sup>21</sup> can weaken the interaction of dye molecules and result in disaggregation of dye molecules. In addition, when using different organic solvents as dispersion medium, they could have diverse effects on dye aggregation. Xia *et al.*<sup>22</sup> found

College of Textiles & Clothing, State Key Laboratory for Biofibers and Eco-textiles, Collaborative Innovation Center for Eco-textiles of Shandong Province, Qingdao University, 308 Ningxia Road, Qingdao 266071, China. E-mail: 13808980221@163.com; chenwc@qdu.edu.cn

† These authors contributed equally to this work.



that reactive dyes formed J-aggregates in the ethanol–water mixture. Wang *et al.*<sup>23</sup> have reported that lactam compounds could inhibit the reactive dyes aggregation. The size of the aggregates in the dye solution has an important effect on the ink droplets of inkjet printing. Some high molecular weight polymers were easily entangle with each other, causing the dye aggregates to be too large and block the nozzle.<sup>24</sup> In fact, surface tension and viscosity are macroscopic behaviours of intermolecular interactions. Surface tension reflects the solute properties at the gas–liquid interface.<sup>25</sup> Viscosity reflects the interaction force between internal molecules.<sup>26</sup> The hydrogen bond between different molecules in the dye solution is one of the factors that cause the dye to aggregate. We studied IR spectroscopy to discuss the hydrogen bond between molecules.<sup>27</sup> We used TEM to study the nano-scale morphology of dye molecules.<sup>28</sup> In this paper, we summarized the previous research experience and investigated the interaction between organic solvents and reactive dyes. Then the effects of hydrophobic groups of organic solvents on dye aggregates were discussed. Finally, we discussed the nano-scale morphology of the dye.

The objective of this work was to understand the effect of three organic solvents *viz* ethylene glycol (EG), ethylene glycol monomethyl ether (MOE), and ethylene glycol dimethyl ether (DME) on aggregation behaviour of reactive Orange 13 dye in order to obtain suitable homogeneous dye solutions for dyeing and printing purpose. The mechanism of interaction between dye molecules and organic solvents were analyzed by performing UV-vis absorption spectrum, fluorescence spectrum, surface tension, rheology and particle size measurements. The role of hydrogen bonding on the solubility of dye dispersions was carried out by IR spectroscopy. The nano-scale morphology of the dye was studied by TEM. We find that, the aggregation behaviour of reactive Orange 13 dye molecules was greatly influenced by the addition of ethylene glycol and its derivatives by disaggregating the dye molecules through hydrophobic effects. It was also found that the surface tension, viscosity and particle size of dye solutions can be changed by the action of the hydrophilic/hydrophobic groups interactions of the ethylene glycol and its derivative. Hydrogen bonding is also one of the reasons for the disaggregation of dye molecules.

## Methods

### Materials

The organic solvents ethylene glycol (EG), ethylene glycol monomethyl ether (MOE), and ethylene glycol dimethyl ether (DME) were purchased from Aladdin Biochemical Technology Co., Ltd. Pure C. I. Reactive Orange 13 (Fig. 1) was purchased from Taiwan Everlight Chemical Industry Co., Ltd.

### Dye solutions preparation

Prepared the mixed solution containing ethylene glycol or its derivatives (EG, MOE or DME), water and Orange 13 dye. First, mixed the water and the organic solvent in proportion (0–50%) to each other. Then, the amount of dye required for the

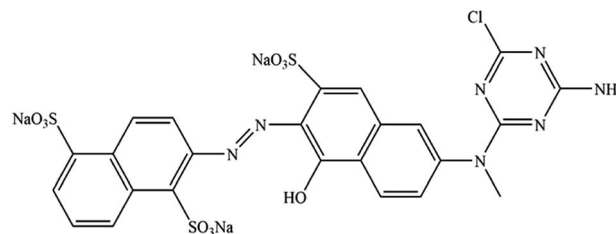


Fig. 1 Chemical structure of Orange 13.

preparation of 100 mM was dissolved in mixed solution at 25 °C and fully stirred until it was completely dissolved. Finally, diluted the dye solution to 50 mM, 10 mM and 1 mM using the mixed solution.

### Measurement of UV-visible absorption spectroscopy

UV-vis absorption spectra of dye solutions with various EG, MOE and DME concentrations over a wavelength range from 250 to 750 nm were recorded by a U-3900H ultraviolet spectrophotometer (Hitachi High-Tech Co., Ltd., Tokyo, Japan) at 25 °C.

### Measurement of fluorescence spectrum

Fluoromax-4 spectrofluorometer (HORIBA Scientific, France) was used to record the fluorescence spectra of dye solutions with various EG, MOE and DME concentrations over a wavelength range from 450 to 750 nm at 25 °C. The excitation wavelength at 380 nm.

Fluorescence quantum yield is a measure of the ability of a substance to emit fluorescence, and is usually expressed by  $\phi$ , which represents the probability that a molecule in an electronically excited state emits fluorescence. At the low concentration dye solutions, the relationship between fluorescence intensity and fluorescence quantum yield and excitation light intensity is as follows:<sup>29,30</sup>

$$F = KI_0cl\epsilon\phi$$

where  $F$  is the fluorescence intensity,  $K$  represents the instrument constant,  $I_0$  is the intensity of the excitation light,  $c$  represents the sample concentration,  $l$  is the optical path of the absorption cell,  $\epsilon$  represents the absorption cell coefficient of the sample and  $\phi$  is the quantum yield. Among them,  $cl\epsilon$  represents the UV optical density  $A$ . If the fluorescence intensities of the two solutions are compared, they have the following relationship:

$$\frac{F_1}{F_2} = \frac{K_1 I_1 c_1 l_1 \epsilon_1 \phi_1}{K_2 I_2 c_2 l_2 \epsilon_2 \phi_2} = \frac{K_1 I_1 A_1 \phi_1}{K_2 I_2 A_2 \phi_2}$$

If the same equipment and test conditions are used, then  $K_1 = K_2$ ,  $I_1 = I_2$ , the formula above can be written as follows:

$$\frac{\phi_1}{\phi_2} = \frac{F_1 A_2}{F_2 A_1}$$



The quantum yield of reactive Orange 13 in the aqueous solution was used as the measurement standard. Using a HORIBA Scientific Fluoromax-4 spectrofluorometer to test the area of the standard and the real emission spectrum of the sample. And a U-3900H UV-vis spectrophotometer was used to test the optical density of standards and samples. This formula can be used to calculate the quantum yield relative to the aqueous solution in each organic solvent.

### Test of dynamic surface tension

Dynamic surface tension of dye solution containing 100 mM Orange 13 and various concentration of EG, MOE and DME were measured using a SITA dynamic surface tension meter (SITA company, Dresden, Germany) at 25 °C. The capillary diameter used in the test is 0.355 mm, and the bubble rupture time ranges from 10 ms to 60 000 ms.

### Determination of rheological property

The rheological property of dye solution containing 100 mM Orange 13 and various concentration of EG, MOE and DME were measured at 25 °C *via* a FLUDICAM RHEO microfluidic visual rheometer (Formulation company, Toulouse, France), the shear rate range is 2000–30 000  $\text{mN s}^{-1}$ .

### Measurement of particle size

Nano ZS90 nanometer particle size analyzer (Malvern Panalytical Ltd, Malvern, UK) was used to measure the particle size of the 100 mM Orange 13 and organic solvents mixed dye solutions at 25 °C.

### Measurement of IR spectra

Since the dye solution contains an aqueous solution, its IR spectrum cannot be measured directly. The dye solution of 100  $\text{mmol L}^{-1}$  was put into a vacuum oven, and its moisture and organic solvent were dried. The IR spectrum of the dye was tested after it is completely dried. IR spectra of dye solutions containing EG, MOE and DME over a wavenumber range from 4000 to 400  $\text{cm}^{-1}$  were record by a NICOLET iS0 IR spectrometer (NICOLET iS0, USA) at 25 °C.

### Measurement of transmission electron microscopy

JEM 2100F Transmission electron microscopy (JEOL company, Japan) were used to photograph the topography of dye molecules at 80 kV. In order to the observation of reactive Orange 13 dye aggregates, a drop of sample solution of Orange 13 dye was placed on 400-mesh formvar copper grids coated with carbon. After the water and solvent evaporate for about 5 minutes, and then observed the surface morphology.

## Results and discussion

### UV-visible absorption spectroscopy

UV-visible absorption spectroscopic technique is an important tool to know the solubility of solutions and understand the interactions between solvent and solute molecules. This section

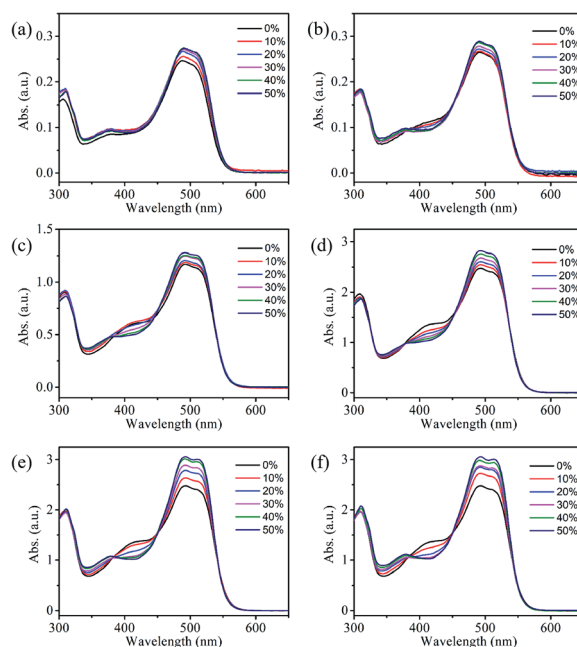


Fig. 2 (a–d) The UV-vis absorption spectra of dye solution containing EG with various reactive Orange 13 concentrations, (a) 1 mM, (b) 10 mM, (c) 50 mM, (d) 100 mM. UV-vis absorption spectra change of dye solutions with different organic solvents concentrations at 25 °C, the Orange 13 concentration is 100 mM, (e) MOE, (d) DME.

will focus on understanding the interaction of reactive Orange 13 dye molecules and three organic solvents. Fig. 2a–d shows that increasing the Orange 13 dye concentrations from 1 mM to 100 mM, the UV-vis absorption spectra changed obviously at monomer peak ( $\lambda_1$ ), dimer peak ( $\lambda_2$ ) and multimers peak ( $\lambda_3$ ) which corresponding to 513 nm, 492 nm and 380–450 nm.<sup>32,33</sup> This is attributed to the probability of the dye molecules colliding with each other increases with the increase of dye concentration. The dye aggregates are affected by the hydrogen bond, van der Waals force, and the  $\pi$ - $\pi$  bond interaction between the dye molecules.

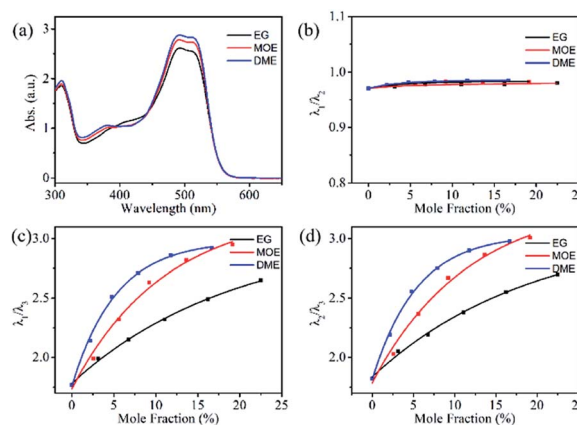


Fig. 3 (a) UV-vis absorption spectra of dye solution containing 100 mM Orange 13 and 30% organic solvent. The ratio of the different absorption peak intensity of the UV-vis absorption spectrum, (b)  $\lambda_1/\lambda_2$ , (c)  $\lambda_1/\lambda_3$ , (d)  $\lambda_2/\lambda_3$ .



Orange 13 has better molecular planarity. Attribute to the thermal movement of the Orange 13 molecules, a multimer cluster structure is formed when the dye molecules are close to each other. The coupling of the  $\pi$  electron cloud of the chromophore groups can cause the  $\pi$  orbital energy levels to split, forming high and low energy levels. Dye molecules generally exist as H-aggregations, which means that after the electrons are excited, the dye molecules could transit to higher energy levels. Since Orange 13 has better molecular planarity, in addition to bimolecular coupling, more intermolecular coupling may occur. This results in a new absorption peak at short wavelengths, and the intensity of the UV-vis absorption peak also enhance with increasing dye concentration (Fig. 2a–d).

In order to understand the interaction between three organic solvents with Orange 13, especially in highly dye concentration solutions, UV-vis absorption spectra were measured as shown in Fig. 2d–f. The intensity of the multimers peak (380–450 nm) gradually decrease with the improvement of the solvent concentration, this indicates that the aggregation of Orange 13 gradually decreases. The dimer peak at 492 nm and monomer peak at 513 nm gradually increase with the increase of the organic solvent, this indicates that the dimers and monomers gradually enhance. It shows that the increasing concentration of organic solvents improves the solubility of Orange 13. As the EG concentration increases, the dye molecules and the solvent molecules are close to each other due to the dispersion force, which may cause relative displacement between the dye molecules and inhibition of dye aggregations. For MOE and DME, it can be seen in Fig. 2e and f that increasing the concentration of organic solvents can also inhibit the aggregation of Orange 13 dye molecules.

As shown in Fig. 3a, adding 30% EG, MOE and DME into the 100 mmol Orange 13 dye solution resulted in an obvious increase of dimer peak at 512 nm and monomer peak at 492 nm. The absorption peak of the DME/Orange 13 solution is higher than MOE/Orange 13 solution, the lowest absorption peak is EG/Orange 13 solution. Fig. 3–d show the ratio of different absorption peak intensity. Compared with the dimer peak (Fig. 3b), the monomer peak has a slight upward trend, while compared with the multimers peak, monomer peak (Fig. 3c) and dimer peak (Fig. 3d) gradually increase, which also proves the disaggregation effect of EG, MOE and DME on Orange 13. This may be due to the increased number of hydrophobic parts in organic solvents. As the hydrophilic hydroxyl groups in organic solvents are replaced by methyl group, the addition of EG, MOE and DME destroyed the ice-like structure between the dye molecules and the water molecules.<sup>34,35</sup> The dispersion force between dye molecules and organic solvent molecules increases with the increase of the number of methyl groups in organic solvent. Stronger dispersion forces lead to more severe damage to the ice-like structure. It also explains that the disaggregation effect becomes more obvious as the number of methyl groups in the solvent increases.

## Fluorescence spectroscopy

Dye aggregates can inhibit the re-emission of fluorescence and affect the fluorescence and quantum yield of the dye solution. Effects of the organic solvents on the dye aggregates were studied through the fluorescence spectra. As shown in Fig. 4, all fluorescence spectra of the three organic solvents showed similar trends, the fluorescence spectrum rises first and then decreases as the increase of organic solvent concentration. With the increase of EG, MOE and DME concentrations, the viscosity gradually increases, and the diffusion movement of the molecules also slow down. Organic solvents increase the solubility of dyes and inhibit the aggregation of dye molecules, resulting in a decrease in dye aggregates and an increase in monomers. The above effects could suppress the non-radiative transition process of the dye molecules, while increasing the probability of radiative transitions could increase the fluorescence intensity.<sup>36–39</sup> The decrease in fluorescence intensity is owing to the continuous increase of organic solvents that may cause the fluorescence of the dye to quench.<sup>31,40–42</sup> Different solvent properties lead to different quenching concentration of dye solution. Fig. 4a–c show that the dye solution quenches when the EG, MOE, and DME concentrations reach 40%, 30%, and 30%. In order to reduce the effect of fluorescence quenching on the fluorescence spectra, the concentration of 1 mM Orange 13 and the ratio of EG, MOE and DME of 30% were selected to make a comparison of three organic solvents. The fluorescence spectra of three organic solvents were compared in Fig. 4d. According to the UV-vis absorption spectra and the fluorescence spectra, the optical density and fluorescence intensity of the UV-vis absorption spectra at the excitation wavelength are calculated, as shown in Table 2.

The dyes in the solutions containing EG, MOE and DME had larger fluorescence quantum yield than that in aqueous solution.

Compared with aqueous solution, the addition of organic solvents can stimulate more dye molecules from multimers to

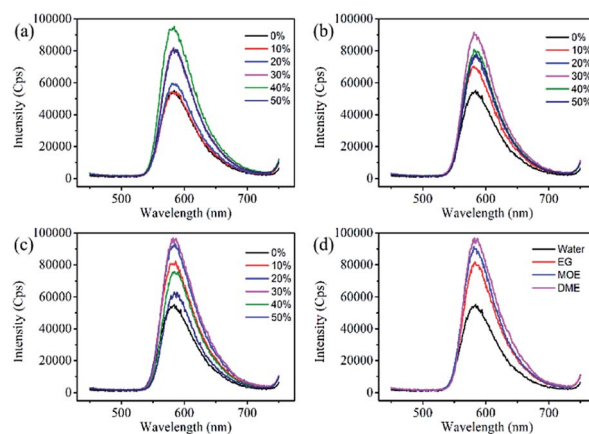


Fig. 4 Fluorescence spectroscopy of 1 mM Orange 13 dye solutions containing EG and its derivatives compounds with different concentrations at 25 °C. (a) EG, (b) MOE, (c) DME. (d) Fluorescence spectrum of 1 mM Orange 13 solution containing 30% organic solvent at 25 °C.



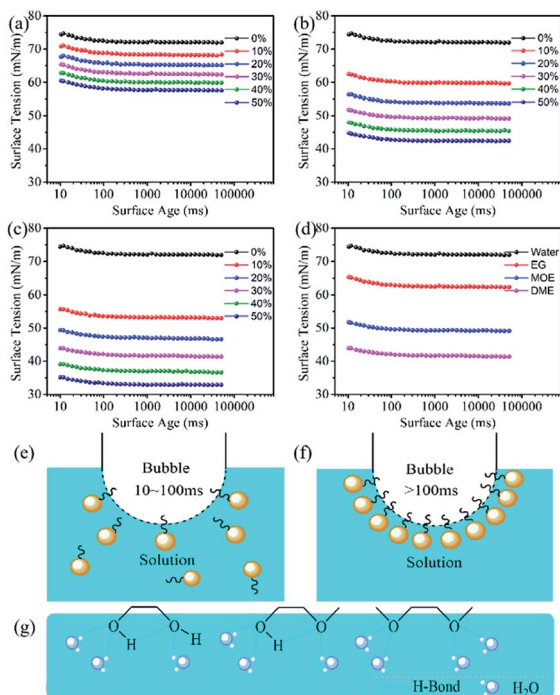


Fig. 5 Surface tensions of dye solutions with EG and its derivatives compounds at 25 °C, the Orange 13 dye concentration is 100 mM. (a) EG, (b) MOE, (c) DME. (d) Surface tension of 100 mM Orange 13 dye solution containing 30% organic solvent at 25 °C. Surface tension of dye solution at different bubble lifetime: (e) 10–100 ms, (f) >100 ms. (g) The arrangement of EG, MOE and DME molecules at the air/water interface.

monomers. Attribute to the hydrophobic interaction between the dye molecules and ethylene glycol and its derivatives, the addition of organic solvents destroys the ice-like structure formed by the water molecules between the dye molecules. Compared with EG, MOE has one more hydrophobic methyl group, and DME has one more methyl group than MOE. The increased hydrophobic methyl group increases the dispersion force of the organic solvent and the dye molecule, and makes the destruction of the ice-like structure by organic solvents more significant. This leads to an increase in monomers in the dye, which increases fluorescence intensity and quantum yield.

### Surface tension

The dynamic surface tension is related to the concentration of solute and solvent at the gas-liquid interface of the dye solution.<sup>43</sup> Fig. 5a–c show the surface tensions of 100 mM Orange 13 dye solutions with three different organic concentration. An interesting phenomenon was that the surface tension of the dye solutions could decrease slowly during the bubble lifetime of 10–100 ms. This may be due to the fact that when the bubble lifetime is less than 100 ms, only a small amount of the solvents or dyes hydrophobic parts can be adsorbed on the gas-liquid interface (Fig. 5e). When the bubble lifetime is longer than 100 ms, the hydrophobic parts of solvents or dyes can arrange at the gas-liquid interface to achieve a stable surface tension (Fig. 5f).

Fig. 5a–c show the change of dye solution surface tension with surface age. The surface tension of the dye solutions containing three different organic solvents gradually decreases with increasing solvent concentration. Because organic solvent has surface activity, the arrangement of solvents at the gas-liquid interface increases with the increase of the EG, MOE and DME concentrations, which could cause the surface tension to decrease. Fig. 5d shows adding 30% EG, 30% MOE or 30% DME into the dye solution resulted in an obvious decrease of surface tension. The dye solution containing EG has the largest surface tension, while the surface tension of the dye solution containing MOE is higher than that of the dye solution containing DME. Fig. 5g shows the arrangement of organic solvents at the gas-liquid interface. When EG is added, the hydrophobic carbon chain could extend out of the liquid phase, causing the surface tension of the dye solution to gradually reduce. As the methyl groups increasing, more hydrophobic groups adsorbed on the air-liquid interface, which resulted in the surface tension decreasing more significantly.<sup>44</sup>

### Rheology

Fig. 6 shows that the viscosity of the dye solution almost does not change with the change of shear rate, which means that all the dye solutions show good Newtonian behaviour.<sup>23</sup> The intermolecular force increases with the increase of organic solvent concentration, as a result, the viscosity of the dye solution gradually increases. Among them, EG has the largest

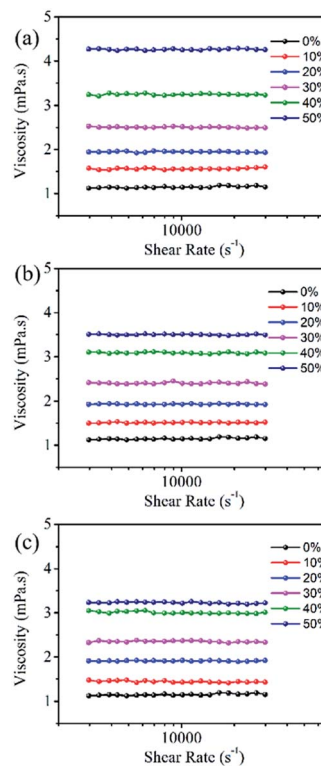


Fig. 6 The rheological property of 100 mM Orange 13 dye aqueous solution containing different organic solvents at 25 °C. (a) EG, (b) MOE and (c) DME.



Table 1 The parameters of organic solvents<sup>a</sup>

| Solvent | Chemical structure   | Hydrogen bonding <sup>a</sup> (kJ mol <sup>-1</sup> ) | molar mass (g mol <sup>-1</sup> ) | Polarity <sup>a</sup> |
|---------|--|---|-----------------------------------|-----------------------|
| EG      | HO-CH <sub>2</sub> -CH <sub>2</sub> -OH                                | 26.0  | 62.07                             | 11.0                  |
| MOE     | HO-CH <sub>2</sub> -CH <sub>2</sub> -O-CH <sub>3</sub>                 | 14.3  | 76.09                             | 9.2                   |
| DME     | H <sub>3</sub> C-O-CH <sub>2</sub> -CH <sub>2</sub> -O-CH <sub>3</sub> | 6.0   | 90.12                             | 6.3                   |

<sup>a</sup> The values of hydrogen bonding and polarity are taken from ref. 31.

Table 2 UV optical density (*A*), fluorescence intensity (*F*) and the quantum yield relative to the aqueous solution ( $\varphi_x/\varphi_w$ ) of different organic solvents at 30% in 1 mM Orange 13 aqueous solution at 25 °C

|                                   | Water | EG     | MOE   | DME    |
|-----------------------------------|-------|--------|-------|--------|
| <i>A</i> (a.u.)                   | 0.153 | 0.146  | 0.155 | 0.148  |
| <i>F</i> (a.u.) × 10 <sup>6</sup> | 4.22  | 6.14   | 6.69  | 7.24   |
| $\varphi_x/\varphi_w$             | 1     | 1.5235 | 1.664 | 1.7746 |

influence on the viscosity of the dye solution, followed by MOE, and DME has the least effect. The viscosity of the dye solution is affected by the interaction forces between molecules such as hydrogen bonds and van der Waals forces. As can be seen from Table 1, EG has the largest hydrogen bonding force because of two hydroxyl groups, this is also one of the factors leading to the highest viscosity of the dye solution containing EG.

### Particle size

There were Orange 13 monomers, dimers and multimers in the dye solution. The particle size of the dyes in the organic solvent-water mixed solution were measured to investigate the interaction between the organic solvents and the dyes.

Fig. 7 shows the particle size of 100 mM Orange 13 dye solutions containing different concentrations of EG and its derivatives. It is obvious in the Fig. 7 that, as the concentration of the organic solvent increases, the particle size of the dyes gradually decreases. This indicates that increasing of concentration of EG and its derivatives could inhibit dye aggregation. Adding same concentration organic solvents into the dye solution resulted in an obvious decrease of particle size, the dye

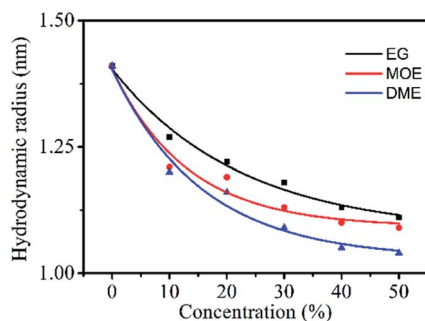


Fig. 7 The particle size (nm) of 100 mM Orange 13 dye solutions containing different concentrations EG and its derivative.

solution containing DME has the smallest particle size and the dye solution containing EG has the largest particle size. This is because EG does not contain methyl groups, which results in minimal impact on dye aggregates. MOE has one more methyl group than EG, which could increase the dispersion force between the dye molecules and the solvent molecules, and enhances the inhibition of Orange 13 aggregates. According to the previous analysis, DME contains two methyl groups, so the disaggregation of Orange 13 is the most obvious. Therefore, we concluded that EG has the minimal inhibiting effect on reactive Orange 13 aggregates, comparing to DME.

### Role of hydrogen bonding in formulation of dye dispersions

Hydrogen-bonding interactions lead to significant changes in the IR spectrums as shown in Fig. 8. In the IR spectra of pure powder dye, the broad and intense peak between 3000–3600 cm<sup>-1</sup> is assigned due to presence of free -OH groups in the dye molecules.<sup>45</sup> Although, the presence of intermolecular hydrogen bonding between dye molecules causes self-association of dye molecules which lead to aggregation and the peak intensity should be less, but in reality, the peak is broad and intense because there are large number of free -OH groups.<sup>46</sup> Upon addition of water and other organic solvents the intensity of peaks decreases which is attributed to the formation of more hydrogen bonding and there will be increase in the solubility of dye molecules. The impact of effect was seen highest in water molecule followed by EG, MOE and DME solvents. The one water molecules form four hydrogen bonds with the four dye molecules and hence in this case there is

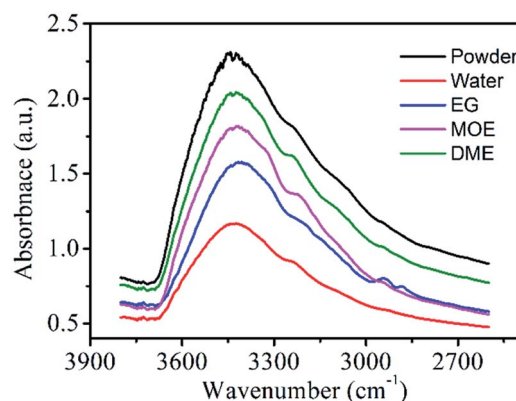


Fig. 8 The IR spectra of dye after evaporation of organic solvent (30%) and water.



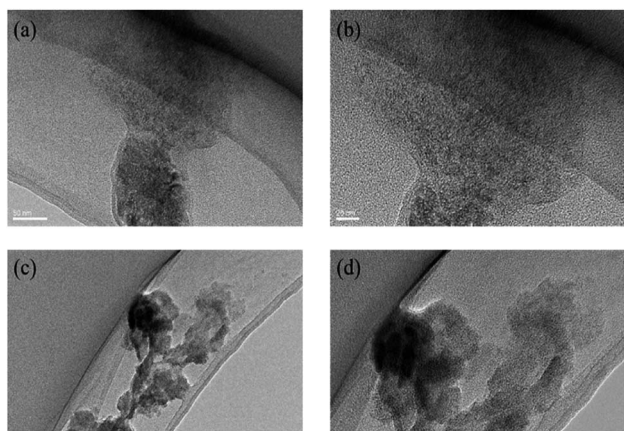


Fig. 9 The TEM of reactive Orange 13 dye molecules in aqueous solution (a) 50 nm, (b) 20 nm. The TEM of reactive Orange 13 dye molecules in 30% MOE–aqueous solution (c) 50 nm, (d) 20 nm.

a smaller number of availabilities of free –OH groups and therefore the peak is less intense. Although because of high polar nature of water the dye molecules should be soluble but the dye molecules are not fully soluble in water because of non-polar groups on the dye molecules. Hence, we select other solvents to make a suitable ink formulation for dyeing and printing purposes. Moreover, it is obvious from the IR peaks that there is slightly shifting of peaks towards shorter wave number means down shift.<sup>47</sup> The reason for this is that on adding water and organic solvents to dye the formation of hydrogen bonding leads to decrease in bond strength between O and H groups of dye molecules.

### Measurement of transmission electron microscopy

The nano-scale morphology of dye molecules was observed by TEM techniques, which is the most intuitive way to observe dye molecules. As shown in Fig. 9a and b, when the  $1 \text{ mmol L}^{-1}$  dye aqueous solution is deposited on the copper mesh, there would be a cluster structure of many dye molecules formed on the copper mesh. The small black dots in the Fig. 9 represent many small nano-scale dye molecules and dye aggregates. Whether in water or in an organic solvent–aqueous solution, the dye solution could form a cluster structure of many dye molecules after deposition.

### Interaction between three solvents with reactive Orange 13 dye

The dispersion force and H-bond was recognized to be one of the main driving forces for the aggregation process.<sup>48–50</sup> Fig. 10a and c show the interaction of Orange 13 in aqueous solution, dimers and even multimers are formed due to the  $\pi$ – $\pi$  interaction of the naphthalene ring between the dye molecules. The benzene ring and ethyl group can result in 23 water molecules and 8 water molecules fixing and forming the ice-like structures (Fig. 10e), respectively,<sup>51,52</sup> which could promote the aggregation of the dye molecules. When EG is added, the naphthalene ring of the dye and the hydrophobic part of the organic solvent may attract each other due to the dispersion force. The ice-like structure of the water molecules was destroyed by the organic solvent, thereby

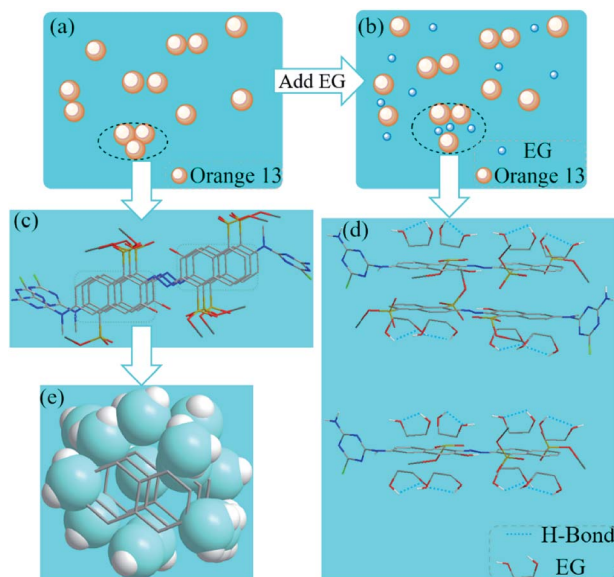


Fig. 10 (a) The Orange 13 molecules in aqueous solution. (b) The Orange 13 molecules in EG solution. (c) The Orange 13 multimer in aqueous solution. (d) Interaction between EG with Orange 13. (e) The ice-like structure in aqueous solution.

suppressing the aggregation of Orange 13 (Fig. 10b and d). In the dye solutions, the strongest force is the attraction between two hydrophobic determinants.<sup>44</sup> More methyl groups lead to a stronger dispersion force of the naphthalene ring between the dye molecule and the organic solvent, which increases the solubility of Orange 13 and inhibits dye aggregation. Therefore, the disaggregation ability of MOE is stronger than EG, and the disaggregation ability of DME is the strongest.

## Conclusions

This study shows that the concentration and structure of organic solvents, especially the structure of the hydrophobic groups in organic solvents, have different effects on the aggregation of reactive dyes. The possibility that the dye molecules collide with each other increases with the increase of the dye concentration, which promotes the aggregation of the dye molecules. The increased concentrations of organic solvent aggravate the relative displacement of the Orange 13 aggregates, so EG, MOE and DME could disaggregate the dye multimers into monomers and dimers at a high concentration. The increased concentrations of organic solvent aggravate the relative displacement of the Orange 13 aggregates. EG, MOE and DME could disaggregate the dye multimers into monomers and dimers. DME can significantly reduce the surface tension and particle size of the dye solution due to more methyl groups in the DME molecules. As for the viscosity is concerned, EG has the greatest influence on the viscosity of the dye solution followed by MOE and DME solvents. IR spectroscopy shows that hydrogen bonding is also one of the reasons for the disaggregation of dye molecules. The nanoscale structure of reactive Orange 13 dye molecules was successfully confirmed by TEM. Therefore, with the increase of the hydrophobic part of the organic solvent, the influence on the dye aggregation become increasingly



evident. This result will provide support for future research on the effect of solvents on the aggregation structure of dyes.

## Conflicts of interest

The authors declare no competing financial interest.

## Acknowledgements

This work is supported by the (1) National Key R&D Program of China, grant no. 2017YFB0309800; and the (2) Shandong Province Key Technology R&D Program, grant no. 2019TSLH0108; (3) State Key Laboratory of Bio-Fibers and Eco-Textiles (Qingdao University), No. ZKT01.

## References

- J. Heier, R. Steiger, R. Hany and F. Nuesch, *Phys. Chem. Chem. Phys.*, 2011, **13**, 15714–15722.
- H. Jiang, X. Li, H. Wang, G. Huang, W. Chen, R. Zhang and R. Yang, *ACS Appl. Mater. Interfaces*, 2020, **12**, 26286–26292.
- X. Li, Z. Liang, H. Wang, S. Qiao, Z. Liu, H. Jiang, W. Chen and R. Yang, *J. Mater. Chem. A*, 2020, **8**, 1360–1367.
- S. Nachimuthu, W. C. Chen, E. G. Leggesse and J. C. Jiang, *Phys. Chem. Chem. Phys.*, 2016, **18**, 1071–1081.
- T. Abe, *Adv. Mater. Res.*, 2012, **441**, 23–27.
- N. J. Buurma, *Curr. Opin. Colloid Interface Sci.*, 2017, **32**, 69–75.
- J. Y. Park, Y. Hirata and K. Hamada, *Dyes Pigm.*, 2012, **95**, 502–511.
- Y. Song, K. Fang, Y. Ren, Z. Tang, R. Wang, W. Chen, R. Xie, Z. Shi and L. Hao, *Polymers*, 2018, **10**, 1402.
- K. Bredereck and C. Schumacher, *Dyes Pigm.*, 1993, **21**, 45–66.
- K. Zhang, R. Xie, K. Fang, W. Chen, Z. Shi and Y. Ren, *J. Mol. Liq.*, 2019, **287**, 110932.
- U. H. Siddiqua, S. Ali, M. Iqbal and T. Hussain, *J. Mol. Liq.*, 2017, **241**, 839–844.
- Z. Tang, K. Fang, Y. Song and F. Sun, *Polymers*, 2019, **11**, 739.
- K. Xie, A. Gao, M. Li and X. Wang, *Carbohydr. Polym.*, 2014, **101**, 666–670.
- R. Xie, K. Fang, Y. Liu, W. Chen, J. Fan, X. Wang, Y. Ren and Y. Song, *J. Mater. Sci.*, 2020, **55**(26), 11919–11937.
- L. Antonov, G. Gergov, V. Petrov, M. Kubista and J. J. T. Nygren, *Talanta*, 1999, **49**, 99–106.
- X. Zhang, K. Fang, H. Zhou, K. Zhang and M. N. Bukhari, *J. Mol. Liq.*, 2020, **312**, 113481.
- M. Dakiky and I. Nmcova, *Dyes Pigm.*, 1999, **40**, 141–150.
- F. Donati, A. Pucci and G. Ruggeri, *Phys. Chem. Chem. Phys.*, 2009, **11**, 6276–6282.
- J. Suesat, *Kasetsart J.: Nat. Sci.*, 2008, **42**, 558–568.
- J. Xiang, X. Yang, C. Chen, Y. Tang, W. Yan and G. Xu, *J. Colloid Interface Sci.*, 2003, **258**, 198–205.
- M. C. Stumpe and H. Grubmüller, *J. Phys. Chem. B*, 2007, **111**, 6220–6228.
- L. Xia, A. Wang, C. Zhang, Y. Liu, H. Guo, C. Ding, Y. Wang and W. Xu, *Green Chem.*, 2018, **20**, 4473–4483.
- R. Wang, K. Fang, Y. Ren, Y. Song, K. Zhang and M. N. Bukhari, *J. Mol. Liq.*, 2019, **294**, 1–7.
- J.-Y. Park, Y. Hirata and K. Hamada, *Color. Technol.*, 2012, **128**, 184–191.
- S. A. Onaizi, *Eur. Biophys. J.*, 2018, **47**, 631–640.
- Y. Ma, H. Yang, J. Guo, L. Wang and J. Zhang, *Theor. Chim. Acta*, 2017, **136**(110), 1–13.
- B. Dereka, J. Helbing and E. Vauthey, *Angew. Chem., Int. Ed. Engl.*, 2018, **57**, 17014–17018.
- H. Wang, Y. Zhang, Y. Chen, H. Pan, X. Ren and Z. Chen, *Angew. Chem., Int. Ed. Engl.*, 2020, **59**, 5185–5192.
- P. G. Wu and L. Brand, *Anal. Biochem.*, 1994, **218**, 1–13.
- K. Zhao, J. Li, H. Wang, J. Zhuang and W. Yang, *J. Phys. Chem. C*, 2007, **111**, 5618–5621.
- C. M. Hansen, *Hansen Solubility Parameters (A User's Handbook, Second Edition) II Solubility Parameters*, 2007.
- A. Ghanadzadeh Gilani, H. Dezhampannah and Z. Poormohammadi-Ahandani, *Spectrochim. Acta, Part A*, 2017, **179**, 132–143.
- D. Takahashi, H. Oda, T. Izumi and R. Hirohashi, *Dyes Pigm.*, 2005, **66**, 1–6.
- S. Okouchi, P. Thanatuksorn, S. Ikeda and H. Uedaira, *J. Solution Chem.*, 2011, **40**, 775–785.
- M. Rueping and T. Theissmann, *Chem. Sci.*, 2010, **1**, 473–476.
- J. Bujdak and N. Iyi, *J. Colloid Interface Sci.*, 2012, **388**, 15–20.
- M. Cigán, J. Donovalová, V. Szöcs, J. Gašpar, K. Jakusová and A. Gáplovský, *J. Phys. Chem. A*, 2013, **117**, 4870–4883.
- B. B. Raju and T. S. Varadarajan, *J. Phys. Chem.*, 1994, **98**, 8903–8905.
- M. Cigan, J. Filo, H. Stankovicova, A. Gáplovsky and M. Putala, *Spectrochim. Acta, Part A*, 2012, **89**, 276–283.
- L. H. Aboud and S. J. Shoja, *Acad. Res. Int.*, 2016, **7**(1), 17–21.
- P. Verma and H. Pal, *J. Phys. Chem. A*, 2013, **117**, 12409–12418.
- F. M. Zehentbauer, C. Moretto, R. Stephen, T. Thevar, J. R. Gilchrist, D. Pokrajac, K. L. Richard and J. Kiefer, *Spectrochim. Acta, Part A*, 2014, **121**, 147–151.
- H. J. J. Staat, A. van der Bos, M. van den Berg, H. Reinten, H. Wijshoff, M. Versluis and D. Lohse, *Exp. Fluids*, 2016, **58**, 1–8.
- C. J. van Oss, D. R. Absolorn and A. W. Neurnann, *Colloid Polym. Sci.*, 1980, **258**, 424–427.
- Z. S. Baird, V. Oja and O. Jarvik, *Appl. Spectrosc.*, 2015, **69**, 555–562.
- W. Zhou, H. Liu, Q. Xu, P. Li, L. Zhao and H. Gao, *Spectrochim. Acta, Part A*, 2020, **228**, 117824.
- M. D. Aljabri, N. M. Gosavi, L. A. Jones, P. P. Morajkar, D. D. La and S. V. Bhosale, *Molecules*, 2019, **24**.
- G. Zhang, X. Zhai, M. Liu, Y. Tang and Y. Zhang, *J. Phys. Chem. B*, 2007, **111**, 9301–9308.
- S. Fazeli, B. Sohrabi and A. R. Tehrani-Bagha, *Dyes Pigm.*, 2012, **95**, 768–775.
- O. I. Mostafa, A. Y. Abd El-Aal, A. A. El Bayaa, H. B. Sallam and A. A. Mahmoud, *J. Chin. Chem. Soc.*, 1995, **42**, 507–513.
- G. Ravishanker, P. K. Mehrotra, M. Mezei and D. L. Beveridge, *J. Am. Chem. Soc.*, 1984, **106**, 4102–4108.
- G. Graziano, *J. Chem. Phys.*, 2013, **139**, 127101.

